5760 *Biochemistry* **2010,** *49,* 5760–5765
DOI: 10.1021/bi100605e

BIOCHEMISTRY
including biophysical chemistry & molecular biology
Article

Using Fluorine Nuclear Magnetic Resonance To Probe the Interaction of Membrane-Active Peptides with the Lipid Bilayer[†]

Benjamin C. Buer,[‡] Jeetender Chugh,[‡] Hashim M. Al-Hashimi,[‡,§] and E. Neil G. Marsh*[,‡,§,∥]

[‡]*Department of Chemistry,* [§]*Department of Biological Chemistry, and* [∥]*Department of Biophysics, University of Michigan, Ann Arbor, Michigan 48109*

Received April 20, 2010; Revised Manuscript Received June 1, 2010

ABSTRACT: A variety of biologically active peptides exert their function through direct interactions with the lipid membrane of the cell. These surface interactions are generally transient and highly dynamic, making them hard to study. Here we have examined the feasibility of using solution phase ^{19}F nuclear magnetic resonance (NMR) to study peptide−membrane interactions. Using the antimicrobial peptide MSI-78 as a model system, we demonstrate that peptide binding to either small unilamellar vesicles (SUVs) or bicelles can readily be detected by simple one-dimensional ^{19}F NMR experiments with peptides labeled with L-4,4,4-trifluoroethylglycine. The ^{19}F chemical shift associated with the peptide−membrane complex is sensitive both to the position of the trifluoromethyl reporter group (whether in the hydrophobic face or positively charged face of the amphipathic peptide) and to the curvature of the lipid bilayer (whether the peptide is bound to SUVs or bicelles). ^{19}F spin echo experiments using the Carr−Purcell−Meiboom−Gill pulse sequence were used to measure the transverse relaxation (T_2) of the nucleus and thereby examine the local mobility of the MSI-78 analogues bound to bicelles. The fluorine probe positioned in the hydrophobic face of the peptide relaxes at a rate that correlates with the tumbling of the bicelle, suggesting that it is relatively immobile, whereas the probe at the positively charged face relaxes more slowly, indicating this position is much more dynamic. These results are in accord with structural models of MSI-78 bound to lipids and point to the feasibility of using fluorine-labeled peptides to monitor peptide−membrane interactions in living cells.

Antimicrobial peptides (AMPs)[1] comprise a diverse family of membrane-active peptides that are found in essentially all multicellular organisms. They are components of the innate immune system and in higher organisms are also implicated in the activation of the adaptive immune response against infection. Although some AMPs have specific intracellular targets (*1*), most exert their antimicrobial activity by binding directly to the membrane and compromising its integrity (*2*, *3*). AMPs make up one class of a growing number of membrane-active peptides that include anticancer and antiviral peptides, cell-penetrating peptides, viral fusion peptides, and venom peptides. For all these classes of peptides, interactions between the membrane lipid bilayer and the peptide are central to their biological functions.

Although highly diverse in sequence and structure, almost all AMPs share the property of being highly amphipathic, with one face of the peptide being hydrophobic and the other face presenting a cluster of positively charged residues (*4*−*6*). The selectivity of AMPs for bacterial membranes arises primarily from electrostatic interactions between the positively charged peptide and the negatively charged phospholipids that predominate in bacterial cell membranes. Eukaryotic membranes, which contain predominantly neutral phospholipids, are usually less susceptible to disruption by AMPs; the presence of cholesterol in eukaryotic membranes also helps prevent membrane disruption by AMPs (*7*). Upon association with the membrane, disruption of the bacterial membrane may proceed through a number of mechanisms, including the formation of pores, membrane thinning, and detergent-like action (*8*, *9*).

Characterizing peptide−membrane interactions is challenging because of the transient nature of these interactions. Furthermore, the peptide may adopt different orientations with respect to the lipid bilayer and different oligomerization states that are concentration-dependent. Detailed structural models derived from solid state nuclear magnetic resonance (NMR) data are available for some AMPs bound to lipid membranes (*10*−*15*); however, these experiments require peptide concentrations that are orders of magnitude higher than their physiologically active range, so it is not clear whether such structures represent biologically active species.

We have previously investigated the effect of incorporating extensively fluorinated amino acids into both α-helical (MSI-78) (*16*) and β-sheet (protegrin) AMPs (*17*). We have shown that fluorination can be used to modulate the biological properties and membrane interactions of these AMPs; in particular, fluorination of MSI-78 resulted in increased potency toward some bacterial strains and protection against proteolysis when bound to lipid vesicles. Other groups have also demonstrated that fluorination is an effective strategy for modulating bioactive peptides (*18*−*20*).

[†]This research was supported by National Science Foundation Grant CHE 0640934 to E.N.G.M.

*To whom correspondence should be addressed: Department of Chemistry, University of Michigan, Ann Arbor, MI 48109-1055. E-mail: nmarsh@umich.edu. Phone: (734) 763-6096. Fax: (734) 615-3790.

[1]Abbreviations: AMP, antimicrobial peptide; TfeG, L-4,4,4-trifluoroethylglycine; MIC, minimum inhibitory concentration; PBS, phosphate-buffered saline solution; POPC, 1-palmitoyl-2-oleoyl-*sn*-glycero-3-phosphatidylcholine; POPG, 1-palmitoyl-2-oleoyl-*sn*-glycero-3-[phospho-*rac*-(1-glycerol)]; DMPC, 1,2-dimyristoyl-*sn*-glycero-3-phosphocholine; DMPG, 1,2-dimyristoyl-*sn*-glycero-3-phospho-(1′-*rac*-glycerol); DHPC, 1,2-dihexanoyl-*sn*-glycero-3-phosphocholine; SUVs, small unilamellar vesicles; CPMG, Carr−Purcell−Meiboom−Gill pulse sequence.

 Published on Web 06/08/2010

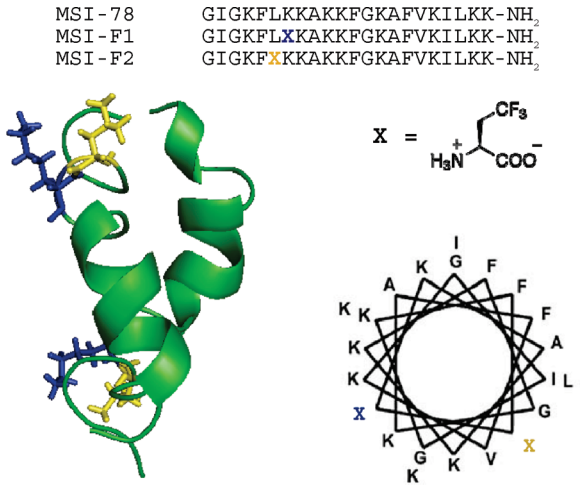

FIGURE 1: Primary sequence of MSI-78 with substitution of Lys in MSI-F1 and Leu in MSI-F2 for trifluoroethylglycine (TfeG). Structure of the MSI-78 dimer in DPC micelles showing the position of amino acid substitutions. Helical wheel diagram illustrating the amino acid substitutions on the hydrophobic and hydrophilic face of MSI-78. The Lys substitution of MSI-F1 is colored blue and the Leu substitution of MSI-F2 yellow.

In this report, we have turned our attention toward using fluorine-containing peptides to probe the interaction of AMPs with membranes by exploiting the sensitive NMR properties of the ^{19}F nucleus. The introduction of fluorine atoms into biological molecules is usually minimally perturbing to structure and function, and fluorine NMR has several advantages for studying biomolecular interactions (*21*, *22*). These include 100% natural abundance and high intrinsic sensitivity, 83% of that of proton NMR, and the high sensitivity of the ^{19}F chemical shift to the local chemical environment. Furthermore, because fluorine is absent from biological molecules, there is minimal background signal.

We have synthesized MSI-78 analogues that incorporate trifluoromethyl groups within their sequence to probe the interaction of the peptide with lipid bilayers. We show that ^{19}F solution NMR can readily be used to detect peptide binding to lipid bilayers and that furthermore the fluorine chemical shift change upon the peptide binding to membranes is sensitive to the position of the probe within the peptide. We have also used ^{19}F CPMG relaxation dispersion experiments to examine the dynamics of the peptide interacting with the membrane.

EXPERIMENTAL PROCEDURES

Peptide Preparation. Racemic 4,4,4-trifluoroethylglycine (TfeG) was purchased from SynQuest Laboratories and enzymatically resolved (porcine kidney acylase I), resulting in L-4,4,4-trifluoroethylglycine having a >99% enantiomeric excess (*23*). The pure amino acid was converted to its t-Boc derivative by standard procedures. The sequences of MSI-78 derivatives are shown in Figure 1. All peptides were synthesized by manual t-Boc procedures on MBHA resin as described previously (*24*, *25*). Peptides were purified with reverse phase HPLC using a gradient of water and acetonitrile with 0.1% TFA; excess residual TFA was removed by a Stratosphere SPE column (Varian). Stock peptide concentrations were determined using ^{19}F NMR with a known concentration of TFA as an internal reference. Peptide identities were confirmed using MALDI-MS.

Lipid Preparation. 1-Palmitoyl-2-oleoyl-*sn*-glycero-3-phosphatidylcholine (POPC), 1-palmitoyl-2-oleoyl-*sn*-glycero-3-phospho-(1′-*rac*-glycerol) (POPG), 1,2-dimyristoyl-*sn*-glycero-3-phosphocholine (DMPC), 1,2-dimyristoyl-*sn*-glycero-3-phospho-(1′-*rac*-glycerol) (DMPG), and 1,2-dihexanoyl-*sn*-glycero-3-phosphocholine (DHPC) were purchased from Avanti Polar Lipids. Fresh POPC/POPG (3:1) SUVs were prepared in PBS buffer (pH 7.4) with 10% D_2O. To make SUVs, multilamellar liposomes were sonicated to clarity using a Fischer Scientific 550 sonic dismembrator, centrifuged to remove insoluble particulates, and used immediately. Isotropic bicelles were made in PBS buffer (pH 7.4) with 10% D_2O via addition of a 3:1 DMPC/DMPG solution to a DHPC solution giving a q of 0.5, resulting in a clear, nonviscous solution.

Circular Dichroism (*CD*). To examine the secondary structure, CD spectra of peptides were recorded with an Aviv 62DS spectropolarimeter at 25 °C. Spectra of peptides in buffered solution and in the presence of SDS micelles were recorded. Mean residue ellipticities, [θ], were calculated using eq 1:

$$[\theta] = \theta_{obsd}/10lcn \quad (1)$$

where θ_{obsd} is the ellipticity in millidegrees, c is the molar concentration, l is the cell path length in centimeters, and n is the number of residues in the protein.

MIC Determinations. The peptide minimum inhibitory concentrations (MICs) against *Escherichia coli* K12 were determined by the microdilution antimicrobial assay procedure, using 96-well plates in replicates of four, as described previously (*26*).

^{19}F NMR. All ^{19}F NMR experiments were performed at 30 °C using a Varian Inova 400 MHz NMR spectrometer equipped with a double-tuned ^{1}H−^{19}F room-temperature probehead. Peptide and lipid samples were prepared with 10% D_2O in PBS (pH 7.4). All experiments were performed at a constant peptide concentration of 400 μM unless indicated otherwise and referenced to trifluoroacetate ion at 0 ppm. ^{19}F CPMG relaxation dispersion experiments were performed for the two peptides in the free state and in the presence of lipid bicelles (200 mM total lipid, q = 0.5, long chain lipids 3:1 mol/mol DMPC/DMPG and short chain lipid being DHPC). CPMG delays (τ_{cp}) were varied from 0.5 to 10.0 ms with each data point recorded as a series of standard one-dimensional transverse relaxation rate measurements with T_2 delays of 0.05, 0.1, 0.2, 0.4, 0.8, and 1.6 ms for free peptide and 0.0125, 0.025, 0.05, 0.1, 0.2, and 0.4 ms for the bicelle-bound peptide. Data sets were recorded with an acquisition time of 1 s in T_1 along with a 10 s prescan delay and 512 scans for a net acquisition time of 2.3−4.6 h/data point. Data were processed and analyzed with VNMRJ and plotted with Origin 8.0.

Theoretical R_2 Calculations. Intrinsic R_2 values for free peptide and peptide bound to bicelles were calculated using eq 2 below (*27*):

$$\frac{1}{T_2} = R_2 = \frac{d^2}{8}[4J(0) + J(\omega_F - \omega_C) + 3J(\omega_C) + 6J(\omega_F) + 6J(\omega_F + \omega_C)] + \frac{c^2}{6}[4J(0) + 3J(\omega_C)] \quad (2)$$

where

$$d = \frac{\mu_0}{4\pi}\gamma_F\gamma_C\frac{h}{2\pi}(r_{CF}^{-3})$$

and

$$c = \frac{\omega_C(\sigma_{||} - \sigma_\perp)}{\sqrt{3}}$$

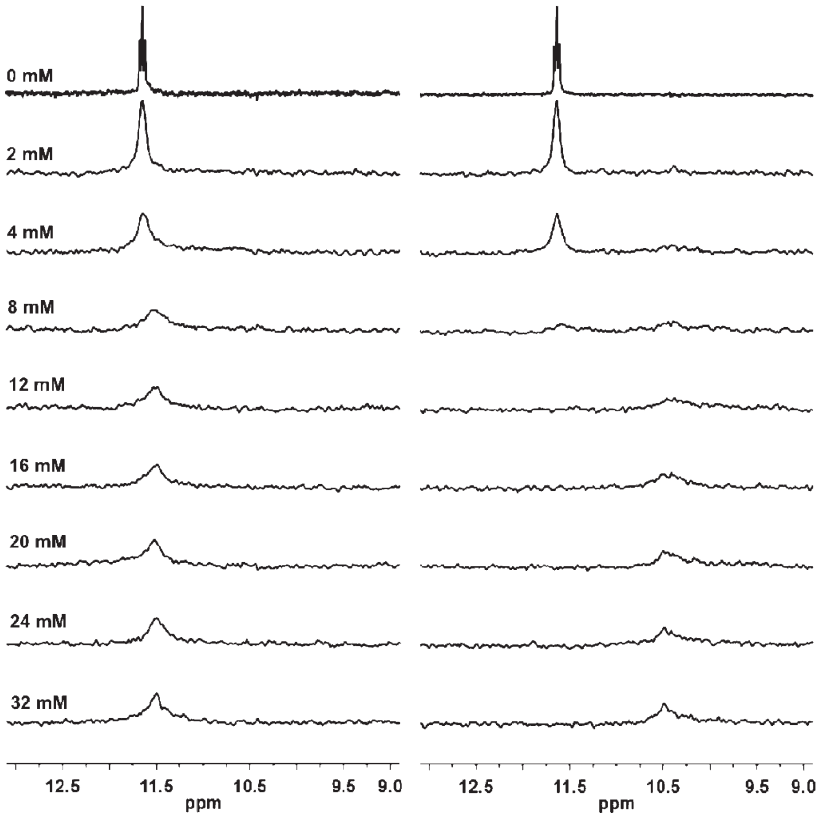

FIGURE 2: ^{19}F NMR spectra of MSI-F1 (left) and MSI-F2 (right) in the presence of increasing concentrations of SUVs. Spectra recorded at 30 °C and pH 7.4 in PBS buffer with 10% D_2O.

$J(\omega)$ in eq 2 is defined as the spectral density at frequency ω and was calculated using eq 3

$$J(\omega) = \frac{2}{5}\left(\frac{S^2\tau_m}{1+\tau_m{}^2\omega^2} + \frac{(1-S^2)\tau}{1+\tau^2\omega^2}\right) \quad (3)$$

where

$$\frac{1}{\tau} = \frac{1}{\tau_m} + \frac{1}{\tau_e}$$

in which μ_0 is the permeability of free space; γ_F and γ_C are gyromagnetic ratios of ^{19}F and ^{13}C, respectively; h is Planck's constant; r_{CF} is the C−F bond length which was taken to be 1.35 Å; ω_C and ω_F are the Larmor frequencies of ^{13}C and ^{19}F, respectively; $\sigma_{\parallel} - \sigma_{\perp}$ is the CSA of the ^{19}F spin and was taken to be 52 ppm (*28*);[2] τ_m and τ_e are correlation times for global and internal motions, respectively; τ_m is assumed to be 1 ns for the free peptide and 20 ns for the peptide bound to bicelles (*29*); τ_e is assumed to be 1 ps; and S^2 is the order parameter that defines the amplitude of the motions and is assumed to be 0.85 for peptides and bicelles.

RESULTS

MSI-78 is thought to disrupt bacterial membranes by forming toroidal pores in the lipid bilayer (*30*). The peptide has been shown to adopt a dimeric α-helical coiled-coil structure in the presence of 3:1 POPC/POPG liposomes in which the dimer interface is formed by contacts between hydrophobic residues and the positively charged lysine residues that face the exterior of the structure and interact with hydrophilic lipid headgroups (*31*). Using this structural model (Figure 1) as a guide, we synthesized variants of MSI-78 in which Lys-7 (MSI-F1) and Leu-6 (MSI-F2) were substituted with trifluoroethylglycine (TfeG). This introduces the CF_3 reporter group into the positively charged exterior and hydrophobic core of the peptide, respectively.

Substitution of TfeG in these peptides does not appear to cause any gross structural changes to the peptides. Both peptides exhibit extensively helical CD spectra in the presence of SDS micelles, and both exhibit MIC values (~4 μg/mL) against *E. coli* K12 strains that are similar to that of the parent MSI-78 peptide (*16*).

We first investigated the interaction of the peptides with small unilamellar vesicles (SUVs), which are often used as a model membrane surface. In free solution at pH 7.4, both MSI-F peptides are unstructured and their ^{19}F NMR spectra exhibit a well-resolved triplet at 11.64 ppm relative to the TFA internal standard (Figure 2). As the peptides are titrated with increasing concentrations of small unilamellar vesicles (SUVs), a new, broadened signal is observed upfield due to the bound peptide. Notably, when they bind SUVs, the chemical shifts of MSI-F1 and MSI-F2 become significantly different, which implies that the CF_3 groups are sampling different chemical environments. The MSI-F1 peak moves upfield by only 0.2 ppm, indicating that the environment of the CF_3 probe at position 7 does not change much. In contrast, the MSI-F2 peak moves upfield by more than 1.0 ppm, suggesting that the CF_3 probe at position 6 experiences a more significantly hydrophobic environment. The degree of peak broadening is also different for the two peptides, with the signal due to MSI-F2 becoming more broadened upon binding to the vesicles.

[2]This is the value measured for 5,5,5-trifluoroleucine, the system closest in structure to TfeG for which CSA has been measured. Although the actual CSA might, of course, be different for TfeG, other CF_3-CH_n-containing compounds for which the CSAs have been measured appear to have similar values which suggests that this approximation is reasonable. For example, the CSA for trifluoroalanine is 44 ppm (*28*); using this value in the calculation yields calculated R_2 values that are ~10% lower.

These observations are consistent with the CF_3 group in MSI-F1 occupying a position at the interface of the peptide with the lipid membrane surface where it may be expected to be in a more polar environment and somewhat more mobile. In contrast, the CF_3 group in MSI-F2 should be buried within the hydrophobic interface of the peptide dimer where its mobility would likely be more restricted.

Titration of the peptides with SUVs also provided an estimate for an apparent dissociation constant for the peptide−membrane complex of approximately 5 mM (assuming 60% of the lipid molecules in the SUVs are available for binding on the outer leaflet of the lipid bilayer).

^{19}F NMR T_2 Analysis of Peptide Binding. The presence of even low concentrations of SUVs results in a marked broadening of the ^{19}F signal of the unbound peptide (Figure 2), suggesting that chemical exchange between the bound and free peptides is occurring on the NMR time scale. Therefore, to investigate the dynamics of the peptide interacting with the lipid bilayer, we decided to measure the transverse relaxation times (T_2) of the CF_3 reporter nuclei as a function of the CPMG pulsing rate ($1/\tau_{cp}$). The relaxation rate, R_{2obs}, as a function of τ_{cp} is given by eq 4 (*32*, *33*):

$$R_{2obs} = \frac{1}{T_{2obs}} = \frac{X_f}{T_{2f}} + \frac{X_b}{T_{2b} + \tau_b} + \tau_b X_b X_f (\delta\omega)^2 \left[1 - \frac{2\tau_b}{\tau_{cp}} \tanh\left(\frac{\tau_{cp}}{2\tau_b}\right)\right] \quad (4)$$

where X_f and X_b are the mole fractions of the free and bound peptide, respectively; T_{2f} and T_{2b} are the transverse relaxation times for free and bound peptide, respectively; τ_b is the residence time for the peptide bound to the lipid; and $\delta\omega$ is the difference in chemical shift between the bound and free peptides. When $\tau_{cp} \ll \tau_b$, the chemical exchange contribution to T_2 is removed and R_{2obs} is independent of τ_{cp}. As τ_{cp} increases to the point that $\tau_{cp} \sim \tau_b$, then R_{2obs} will increase as chemical exchange begins to contribute to relaxation. When $\tau_{cp} \gg \tau_b$, the contribution from chemical exchange reaches an asymptotic limit (maximum); however, the sensitivity of the experiment is significantly diminished as τ_{cp} increases. The maximum τ_{cp} value in a CPMG experiment is limited by evolution under the one-bond scalar coupling Hamiltonian. Increasing τ_{cp} leads to interconversion between in-phase and antiphase magnetization during the spin-echo period as well as loss of signal intensity due to chemical exchange, which in turn leads to large errors in R_{2obs}.

SUVs proved to be insufficiently stable over the longer time periods needed to perform the CPMG measurements. Therefore, we examined the binding of MSI-F1 and MSI-F2 to lipid bicelles, another commonly used model membrane system. Bicelles have the advantage of being more stable than SUVs, and although higher lipid concentrations are needed to form them, they may be considered better mimics of the cell membrane because, unlike SUVs, they are not highly curved. Interestingly, compared with SUVs, the MSF-F1 peptide exhibits a much greater change in chemical shift on binding to bicelles, shifting upfield by ~0.4 ppm. Similarly, the signal due to MSI-F2 shifts upfield by 1.6 ppm on binding to bicelles (Figure 3).

The R_2 ($=1/T_2$) values were measured for both peptides, in free solution and bound to bicelles, for $1/\tau_{cp}$ values ranging from 100 to 2000 Hz. In free solution, both peptides are characterized by an R_{2f} of ~3 Hz which, as expected, is independent of the CPMG pulsing rate and is consistent with the CF_3 group being highly mobile in the unstructured peptide. The experiment was then performed with MSI-F1 and MSI-F2 bound to high concentrations of lipid bicelles, so that contribution to R_{2obs} due to the free peptide is minimal and thus $R_{2obs} = R_{2b}$. For both MSI-F1 and MSI-F2, R_{2b} remains constant for pulsing rates between 200 and 2000 Hz, and only at longer pulse intervals does R_{2b} appear to increase. However, at these time scales, the experiment approaches the limits of sensitivity and measurements are consequently accompanied by a large uncertainty in the value of R_{2b}. Although the data cannot be reliably fit to eq 4 to allow τ_b to be calculated, the experiment does allow us to put an upper limit of ~200 s^{-1} on the rate at which the peptide dissociates from the membrane ($1/\tau_b$).

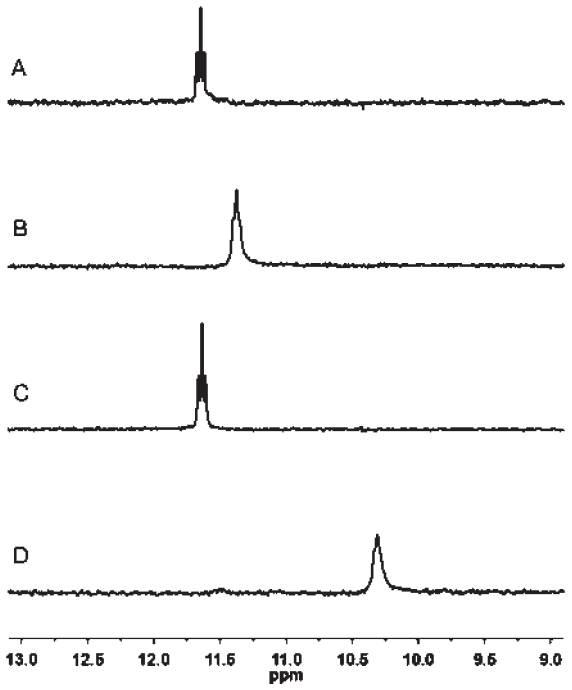

FIGURE 3: ^{19}F NMR spectral changes associated with MSI-F1 and MSI-F2 binding to bicelles: (A) 400 μM MSI-F1, (B) 400 μM MSI-F1 in the presence of 200 mM bicelles, (C) 400 μM MSI-F2, and (D) 400 μM MSI-F2 in the presence of 200 mM bicelles. Spectra were recorded at 30 °C and pH 7.4 in PBS buffer with 10% D_2O and referenced to TFA.

At high CPMG pulsing rates, R_{2b} for the peptides represents the intrinsic relaxation rate of the ^{19}F nucleus with the chemical exchange component removed. The difference between R_{2b} for MSI-F1 (18 ± 1 Hz) and MSI-F2 (35 ± 4 Hz) is significant and may be attributed to differences in the dynamics of the peptide at the two positions monitored by the probe. To gain insights into these differences, the R_2 values were calculated, as described in Experimental Procedures, for the peptides in free solution and when bound to bicelles.

In free solution, the calculated value for R_{2f} of 3.22 Hz, which assumes the peptides are unstructured, agrees very well with the experimentally determined R_{2f} for MSI-F1 and MSI-F2 (Figure 4). Interestingly, however, in the bound state whereas the calculated value for R_{2b} of 38.9 Hz is in excellent agreement with that measured for MSI-F2, it is significantly larger than that measured for MSI-F1 (Figure 4). The lower R_{2b} for MSI-F1 suggests that the CF_3 probe at position 7 is more mobile than if it were tumbling at the correlation time of the bicelle, although not as mobile as in free solution. These observations are in accord with a model that

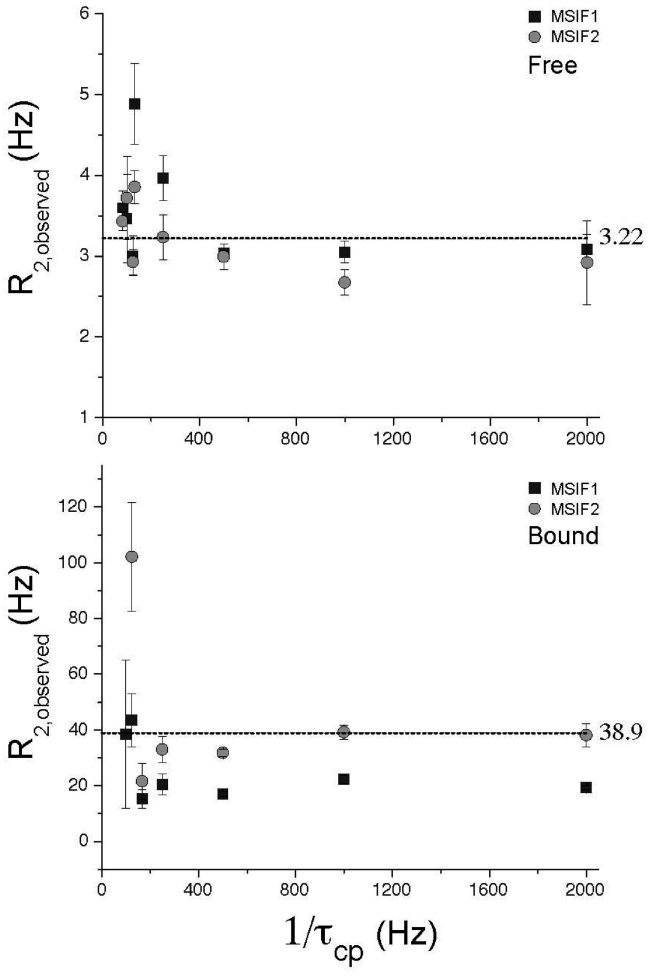

FIGURE 4: Observed transverse relaxation rate, R_{2obs}, plotted as a function of CPMG pulsing rate (ν_{cp}). Data are for MSI-F1 (squares) and MSI-F2 (circles) in buffered solution as unstructured peptides (top) and bound to 200 mM bicelles (bottom). The calculated R_2 values for free peptide and peptide bound to bicelles are indicated by the dashed lines.

places the CF_3 group in MSI-F1 close to the solvent-exposed lipid headgroups, where the side chains may be expected to exhibit greater conformational mobility. In contrast, the model places the CF_3 group in MSI-F2 in the hydrophobic core of the peptide dimer; here the side chain is immobile, and R_{2b} is dominated by the tumbling motion of the bicelle.

DISCUSSION

These experiments demonstrate that fluorine NMR can be used as a sensitive probe to investigate the interactions of peptides with membranes. The ^{19}F nucleus is intrinsically very sensitive and 100% abundant and exhibits wide chemical shift dispersion. Moreover, fluorinated probes can readily be incorporated into peptides site specifically and in a nondisruptive manner as many fluorinated analogues of amino acids are commercially available or easily synthesized. Our experiments were routinely conducted using peptide concentrations of 400 μM to facilitate R_2 measurements; however, these peptides can be detected binding to bicelles at much lower concentrations: 40 μM peptide readily detected at a signal-to-noise ratio of 4:1 at 376 MHz after 512 scans in a spectrum that takes ~15 min to acquire. (With a newer spectrometer operating at higher field strengths and modern cryogenic probes, the sensitivity would be significantly improved.) This potentially allows one to study membrane−peptide interactions using this technique at the concentration range at which they exert their biological activity.

We demonstrated that the fluorine chemical shift is sensitive to both the position of the probe with respect to the membrane surface and, unexpectedly, the nature of the lipid bilayer, larger changes in chemical shift being observed upon binding to bicelles than upon binding to SUVs. This suggests that the peptides interact slightly differently with these two systems. One explanation is that the binding interaction is sensitive to membrane curvature: SUVs, being spherical, exhibit positive curvature of the bilayer and are relatively rigid, whereas bicelles, being disklike, present a flat surface that is more flexible. The difference in membrane topology may well result in subtle changes to the structure of the peptide−membrane complex.

In addition to monitoring peptide binding, NMR also provides information about the dynamics of the peptide−membrane interaction, which would be hard to obtain by other methods. The relaxation measurements show that buried and solvent- or lipid headgroup-exposed positions within the peptide exhibit significantly different dynamics. Whereas the buried position appears to tumble at the frequency of the bicelle, the exposed positions are significantly more dynamic.

To date, solid state NMR of isotopically labeled peptides oriented in lipid bilayers has provided the most detailed information about dynamic aspects of peptide−membrane interactions (*34*), including topological equilibria associated with the orientation of peptides relative to the membrane, the rates of lateral and rotational diffusion, and the oligomerization state of the peptides. The disadvantages of this technique include the high concentrations of peptide required (1−2 mol %), long experimental acquisition times, and the specialized nature of solid state NMR instrumentation. In contrast, solution state measurements are far more routinely made and spectra may be acquired more rapidly. Our experiments are not designed to yield detailed orientation information but to provide sensitive and rapid detection of peptide−membrane interactions and dynamics that could be applied under more physiological conditions.

In conclusion, these studies demonstrate the utility of ^{19}F NMR for investigating the interactions of peptides and proteins with their membrane targets. In particular, the high sensitivity and lack of background signal point to the feasibility of using fluorine NMR to study peptide−membrane interactions in vivo at physiologically relevant concentrations.

REFERENCES

1. Brogden, K. A. (2005) Antimicrobial peptides: Pore formers or metabolic inhibitors in bacteria? *Nat. Rev. Microbiol. 3*, 238–250.
2. Huang, H. W., Chen, F.-Y., and Lee, M.-T. (2004) Molecular mechanism of peptide-induced pores in membranes. *Phys. Rev. Lett. 92*, 198304.
3. Oren, Z., and Shai, Y. (1998) Mode of action of linear amphipathic α-helical antimicrobial peptides. *Biopolymers 47*, 451–463.
4. Hancock, R. E. W., and Lehrer, R. (1998) Cationic peptides: A new source of antibiotics. *Trends Biotechnol. 16*, 82–88.
5. Shai, Y. (1999) Mechanism of the binding, insertion and destabilization of phospholipid bilayer membranes by α-helical antimicrobial and cell non-selective membrane-lytic peptides. *Biochim. Biophys. Acta 1462*, 55–70.
6. Wu, M. H., Maier, E., Benz, R., and Hancock, R. E. W. (1999) Mechanism of interaction of different classes of cationic antimicrobial peptides with planar bilayers and with the cytoplasmic membrane of *Escherichia coli*. *Biochemistry 38*, 7235–7242.
7. Epand, R. F., Ramamoorthy, A., and Epand, R. M. (2006) Membrane lipid composition and the interaction with Pardaxin: The role of cholesterol. *Protein Pept. Lett. 13*, 1–5.

8. Oren, Z., and Shai, Y. (1997) Selective lysis of bacteria but not mammalian cells by diastereomers of melittin: Structure-function study. *Biochemistry 36*, 1826–1835.
9. Selsted, M. E., Novotny, M. J., Morris, W. L., Tang, Y. Q., Smith, W., and Cullor, J. S. (1992) Indolicidin, a Novel Bactericidal Tridecapeptide Amide from Neutrophils. *J. Biol. Chem. 267*, 4292–4295.
10. Ramamoorthy, A., Thennarasu, S., Lee, D. K., Tan, A. M., and Maloy, L. (2006) Solid-state NMR investigation of the membrane-disrupting mechanism of antimicrobial peptides MSI-78 and MSI-594 derived from magainin 2 and melittin. *Biophys. J. 91*, 206–216.
11. Porcelli, F., Verardi, R., Shi, L., Henzler-Wildman, K. A., Ramamoorthy, A., and Veglia, G. (2008) NMR structure of the cathelicidin-derived human antimicrobial peptide LL-37 in dodecylphosphocholine micelles. *Biochemistry 47*, 5565–5572.
12. Powers, J. P. S., Tan, A., Ramamoorthy, A., and Hancock, R. E. W. (2005) Solution structure and interaction of the antimicrobial polyphemusins with lipid membranes. *Biochemistry 44*, 15504–15513.
13. Porcelli, F., Buck, B., Lee, D. K., Hallock, K. J., Ramamoorthy, A., and Veglia, G. (2004) Structure and orientation of pardaxin determined by NMR experiments in model membranes. *J. Biol. Chem. 279*, 45815–45823.
14. Mani, R., Cady, S. D., Tang, M., Waring, A. J., Lehrer, R. I., and Hong, M. (2006) Membrane-dependent oligomeric structure and pore formation of β-hairpin antimicrobial peptide in lipid bilayers from solid-state NMR. *Proc. Natl. Acad. Sci. U.S.A. 103*, 16242–16247.
15. Wu, X., Mani, R., Tang, M., Buffy, J. J., Waring, A. J., Sherman, M. A., and Hong, M. (2006) Membrane-Bound Dimer Structure of a β-Hairpin Antimicrobial Peptide from Rotational-Echo Double-Resonance Solid-State NMR. *Biochemistry 45*, 8341–8349.
16. Gottler, L. M., Lee, H. Y., Shelburne, C. E., Ramamoorthy, A., and Marsh, E. N. G. (2008) Using fluorous amino acids to modulate the biological activity of an antimicrobial peptide. *ChemBioChem 9*, 370–373.
17. Gottler, L. M., De la Salud-Bea, R., Shelburne, C. E., Ramamoorthy, A., and Marsh, E. N. G. (2008) Using fluorous amino acids to probe the effects of changing hydrophobicity on the physical and biological properties of the β-hairpin antimicrobial peptide protegrin-1. *Biochemistry 47*, 9243–9250.
18. Hsieh, K. H., Needleman, P., and Marshall, G. R. (1987) Long-Acting Angiotensin-II Inhibitors Containing Hexafluorovaline in Position-8. *J. Med. Chem. 30*, 1097–1100.
19. Wang, P., Tang, Y., and Tirrell, D. A. (2003) Incorporation of trifluoroisoleucine into proteins in vivo. *J. Am. Chem. Soc. 125*, 6900–6906.
20. Meng, H., and Kumar, K. (2007) Antimicrobial Activity and Protease Stability of Peptides Containing Fluorinated Amino Acids. *J. Am. Chem. Soc. 129*, 15615–15622.
21. Danielson, M. A., and Falke, J. J. (1996) Use of F-19 NMR to probe protein structure and conformational changes. *Annu. Rev. Biophys. Biomol. Struct. 25*, 163–195.
22. Gakh, Y. G., Gakh, A. A., and Gronenborn, A. M. (2000) Fluorine as an NMR probe for structural studies of chemical and biological systems. *Magn. Reson. Chem. 38*, 551–558.
23. Tsushima, T., Kawada, K., Ishihara, S., Uchida, N., Shiratori, O., Higaki, J., and Hirata, M. (1988) Fluorine-Containing Amino-Acids and Their Derivatives. 7. Synthesis and Antitumor-Activity of α-Substituted and γ-Substituted Methotrexate Analogs. *Tetrahedron 44*, 5375–5387.
24. Lee, H. Y., Lee, K. H., Al-Hashimi, H. M., and Marsh, E. N. G. (2006) Modulating protein structure with fluorous amino acids: Increased stability and native-like structure conferred on a 4-helix bundle protein by hexafluoroleucine. *J. Am. Chem. Soc. 128*, 337–343.
25. Gottler, L. M., de la Salud-Bea, R., and Marsh, E. N. G. (2008) The Fluorous Effect in Proteins: Properties of α4F6, a 4-α-Helix Bundle Protein with a Fluorocarbon Core. *Biochemistry 47*, 4484–4490.
26. Shelburne, C. E., An, F. Y., Dholpe, V., Ramamoorthy, A., Lopatin, D. E., and Lantz, M. S. (2007) The spectrum of antimicrobial activity of the bacteriocin subtilosin A. *J. Antimicrob. Chemother. 59*, 297–300.
27. Dalvit, C. (2007) Ligand- and substrate-based F-19 NMR screening: Principles and applications to drug discovery. *Prog. NMR Spectrosc. 51*, 243–271.
28. Grage, S. L., Durr, U. H. N., Afonin, S., Mikhailiuk, P. K., Komarov, I. V., and Ulrich, A. S. (2008) Solid state F-19 NMR parameters of fluorine-labeled amino acids. Part II: Aliphatic substituents. *J. Magn. Reson. 191*, 16–23.
29. Andersson, A., Almqvist, J., Hagn, F., and Maler, L. (2004) Diffusion and dynamics of penetratin in different membrane mimicking media. *Biochim. Biophys. Acta 1661*, 18–25.
30. Hallock, K. J., Lee, D. K., and Ramamoorthy, A. (2003) MSI-78, an analogue of the magainin antimicrobial peptides, disrupts lipid bilayer structure via positive curvature strain. *Biophys. J. 84*, 3052–3060.
31. Porcelli, F., Buck-Koehntop, B. A., Thennarasu, S., Ramamoorthy, A., and Veglia, G. (2006) Structures of the dimeric and monomeric variants of magainin antimicrobial peptides (MSI-78 and MSI-594) in micelles and bilayers, determined by NMR spectroscopy. *Biochemistry 45*, 5793–5799.
32. Dubois, B. W., and Evers, A. S. (1992) F-19-Nmr Spin Spin Relaxation (T2) Method for Characterizing Volatile Anesthetic Binding to Proteins: Analysis of Isoflurane Binding to Serum-Albumin. *Biochemistry 31*, 7069–7076.
33. Luz, Z., and Meiboom, S. (1963) Nuclear Magnetic Resonance Study of Protolysis of Trimethylammonium Ion in Aqueous Solution: Order of Reaction with Respect to Solvent. *J. Chem. Phys. 39*, 366–370.
34. Salnikov, E., Aisenbrey, C., Vidovic, V., and Bechinger, B. (2010) Solid-state NMR approaches to measure topological equilibria and dynamics of membrane polypeptides. *Biochim. Biophys. Acta 1798*, 258–265.